Universiti Malaysia Terengganu Journal of Undergraduate Research *eISSN: 2637-1138*
Volume 2 Number 2, April 2020: 1-8 *© Penerbit UMT*

SYNTHESIS OF ZINC OXIDE NANOPARTICLES BY USING ALOE VERA LEAF EXTRACT AS PONTENTIAL ANODE MATERIAL IN LITHIUM ION BATTERY

SITI RABIATUL ADAWIYAH MAZLI[1], HANIS MOHD YUSOFF[1,2*] AND NURUL HAYATI IDRIS[3]

[1]*Faculty of Science and Marine Environment, Universiti Malaysia Terengganu, 21030 Kuala Nerus, Terengganu, Malaysia.*

[2]*Advanced Nano Materials (ANoMa) Research Group, Faculty of Science and Marine Environment, Universiti Malaysia Terengganu, 21030 Kuala Nerus, Terengganu, Malaysia.*

[3]*Faculty of Ocean Engineering Technology and Informatics, Universiti Malaysia Terengganu, 21030 Kuala Nerus, Terengganu, Malaysia.*

**Corresponding author: hanismy@umt.edu.my*

Abstract: Synthesis of nanoparticles by using plant have sparked interest among researchers due to environmentally safe, inexpensive and simple method to compare with chemical method. Use of plant in synthesis zinc oxide nanoparticles (ZnO NPs) that act as reducing and capping agent are more recommended, due to high production of product and rate of synthesis is faster than using microorganism. This study focus on the synthesis of ZnO NPs by using leaf extract of aloe vera (*Aloe bardenisis miller*) with different concentration (30%, 40% and 50%) and various calcination temperature which are 500 ˚C, 700 ˚C and 900 ˚C for 4 hours. Fourier – transform infrared spectroscopy (FTIR), Thermogravimetric Analysis (TGA), scanning electron microscopy (SEM), X-ray Diffraction (XRD) and Brunauer-Emmet and Teller (BET) were used to characterize the prepared samples. FTIR spectra showed present wavenumber in between 400-500 cm^{-1} indicated the presence of Zn-O stretch. Powder XRD pattern confirmed the hexagonal wurtzite structure with average particles size from 24.19 nm to 67.69 nm for all concentration and temperature by using Scherer's equation. For SEM analysis the images show irregular shape for concentrations 30% and 50% with size range from 500 nm to 900 nm while for concentration 40% cubic shape was observe with size range from 140 nm to 900 nm. All characterize show that formation of ZnO NPs depend on the concentration and calcination temperature. Sample 30% and 50% ZnO NPs was applied in lithium battery at voltage from 0.01 to 3. 1.2 $mAhg^{-1}$ was recorded for sample 30% ZnO NPs while 100 $mAhg^{-1}$.

Keywords: Zinc Oxide Nanoparticles, lithium ion battery, green synthesis, Aloe vera

Introduction

Green synthesis of zinc oxide nanoparticles (ZnO NPs) have triggered interest among researcher due to unique chemical and physical properties and high demand due to variety of applications in industry production. ZnO NPs known as atom- like behavior due to high and huge explicit surface area, high division of surface molecules and conduction band when divided to near atomic size (Jacobsson *et al*., 2014). Most of ZnO NPs are synthesize by using chemical method. Nevertheless, chemical synthesis methods require different physical and chemical processes are currently widely used to synthesize metal nanoparticles, which allow one to obtain particles with the desired characteristics. However, the chemical methods require numerous dangerous and perilous synthetic substances that are costly and unsafe to living being. Therefore, nowadays many researchers attracted to green and biological method due to the cost-effective, feasibility, less toxic nature process and environmental friendly. Plants extract seem to be the best media. This is because, large scale biosynthesis of nanoparticles would produce (Iravani *et al.,* 2011).

Recently synthesis ZnO NPs by using green synthesis had been performs in previous studies. However their several properties of ZnO NPs that need to discover. In this study, focusing in synthesis ZnO NPs by using green method with different concentration (30%, 40% and 50% of aloe vera leaf extract) and temperature (500 ˚C, 600 ˚C and 700 ˚C). From the previous study, synthesis of ZNO NPs by using aloe vera leaf extract are mostly applied in biological application such as UV protection (Smijs & Paula *et al*., 2011), antibacterial (Ali *et al*., 2016) and food packaging (Espitia *et al.,* 2016), but not in reserving energy application such as potential anode material in lithium ion battery (LIBs).

LIBs had been choose due to their superior performance characteristics, namely, long cycle life, high energy and power densities and no memory effect (Yang *et al*., 2016). Therefore, lithium ion battery mostly apply in laptop and mobile phone as power storage technology (Qi *et al*., 2017). LIBs also certainly plays a central role, as it allows energy savings in terms of fossil fuels by powering electric vehicles and might promote the expansion of renewable energy (Liu *et al*., 2011). ZnO was choose as potential anode in lithium ion battery due to higher theoretical capacity (978 $mAhg^{-1}$) rather than graphite (372 $mAhg^{-1}$) (Xu *et al*., 2014). In addition due to their abundant, non-hazardous, and low cost that contribute ZnO as an active material for LIBs anodes (Wan *et al.,* 2018). Unfortunately, during lithium/delithium process, poor electronic conductivity was produce resulting to poor application (Huang *et al*., 2011). Therefore, to improve the cyclic performance of LIBs, by applying ZnO NPs as active would produce desirable goal, in terms of safety as well as energy and power density (Bresser *et al*., 2013).

Materials and Methods

Preparation of Aloe Vera Extract (ALE)

About 20 g portions of aloe vera leaves were washed by using distilled water and finely cut by using knife that had been rinsed with ethanol. Then, aloe vera leaf was boil with de-ionized water in medium flame (60 °C) for 10 min. The color of extraction changes from watery to light green. The extract cool at room temperature, filter by using Whatman filter paper no 1 and store in refrigerator at 4 °C for future use.

Synthesis of Zinc Oxide nanoparticles (ZNO NPs) by using ALE

Zinc sulfate heptahydrate ($ZnSO_4$. $7H_2O$) and aloe vera extract (ALE) that been used in this method Firstly, ALE were divided into varying concentrations (30, 40 and 50%), were added into 100 ml of 0.25 M $ZnSO_4$.$7H_2O$ solution in different glass flask. Then, 0.1 M was NaOH added until it reach pH 8 and measured by using pH meter. The reaction mixture was kept under vigorous stirring at 60 °C for 3 h. The precipitate obtained was centrifuged at 4500 rpm for 10 minutes, thoroughly washed and dried at 80 °C for 24 h and calcined at 500 ˚C, 700 ˚C and 900 ˚C. The resultant dried material was in powder form and stored in an airtight container.

Fabrication of Super capacity Electrode

First, the copper foil wan rinsed in acetone for 15-20 min and dried by using tissue. Then, the synthesized ZnO NPs act as active material was mixed with carbon black and PVDF were weighed: 0.015 g, 0.004 g and 0.001 g and a drop of 1-methyl-2-pyrrolidone (NMP) was added and the mixture was grind for 15 min using pestle and mortar. The homogenous slurry was pasted on copper foil (1 x 1 cm^2) and dry under vacuum at 100 ˚C for 6 h. Weight range for active material must be around 0.5- 1.0 mg in dried form.

Electrochemical Performance

The preparation of electrochemical performance was performed in ga love box. The coin cells contained ZnO NPs electrode as anode, a lithium foil as reference counter electrode and 1 M $LiPF_6$. First, the lithium foil was added in the coin, then three drop of 1 M of $LiPF_6$ was added in a 1:1 ethyl carbonate (EC): dimethyl

carbonate (DMC) solvent as electrolyte, using celgard 2300 PE membrane as separator. A drop of $LiPF_6$ was added in the coin to activate ion in anode. The copper foil that contain carbon paste was put on the separator. A 9 mm disk was compressed by using clapping machine. NEWARE BTS battery testers was used to monitor the cycling and rate performance of the coin cells were tested with cut-off potential window of 0.01-3.0 V versus the Li+/Li electrode was tested to see the electrochemical performance at different current densities.

Results and Discussion

White powder of ZNO NPs was successfully synthesized with pH 8. During the synthesis process, the color of the solution was changed from yellowish to white precipitate that indicating the ZnO NPs formation. Not only have that, yield of ZnO NPs was also influenced by the concentration of extracted ALE. The higher concentration of ALE used, the higher product yield was produced. In this study, sample using 50% ALE produced the highest yield of product.

TGA analysis was used to measures the weight change of 30%, 40% and 50% ZnO-ALE before calcination by using temperature range from 30 ˚C until 900 ˚C in N_2 environment.

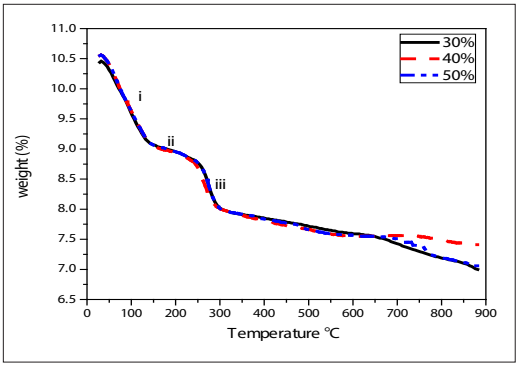

Figure 1: TGA analysis for 30%, 40% and 50% ZnO NPs

Figure 1 shows the degradation started from 30 until 140 ˚C for all samples indicated detach waste that had been absorb in ZnO. For second degradation, removed of water absorbed in ZnO and the final degradation occur due to decomposition of hydroxyl group. All samples show seems not fully completely decompose due to the presence of small amount of organic material (Hassan *et al.,* 2018). This show that all sample require higher energy to completely decompose.

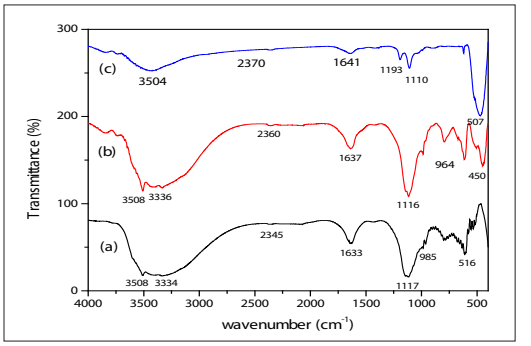

Figure 2: FTIR spectra of ZnO Nps with 30% concentration of ALE and calcined at temperature (a) 500 ˚C, (b) 700 ˚C and (c) 900 ˚C

As shown in Figure 2, all spectra showed a broad peak around 3508 cm^{-1} and 3504 cm^{-1} indicate –OH group from phenol that present in aloe vera leaf extract, while wavenumber at 3334 cm^{-1} and 2345 cm^{-1} that appeared in the 30% ALE ZnO NPs at temperature 500 ˚C were assigned to the stretching vibration of amines (C-N). For wavenumber at 1633 cm^{-1}, 1637 cm^{-1} and 1641 cm^{-1} give the similar band pattern present in characterize of aloe vera leaf extract indicated the presence of carboxylic group (ketone) C=O. Stretching band at 900 cm^{-1} and 1993 cm^{-1} represent the C-O and stretching vibration of aliphatic and aromatic amines (C-N) (Sangeetha *et al.,* 2015). All ZnO NPs exhibit at 516 cm^{-1}, 450 cm^{-1} and 507 cm^{-1} wavenumber show to banding vibration of Zn-O, according to Sanggetha et al., 2015, the peak region of Zn-O vibration mode is located between 600 cm^{-1} until 400 cm^{-1}. FTIR spectra for 40% and 50% of ALE also showed similar pattern obtained for 30% ALE.

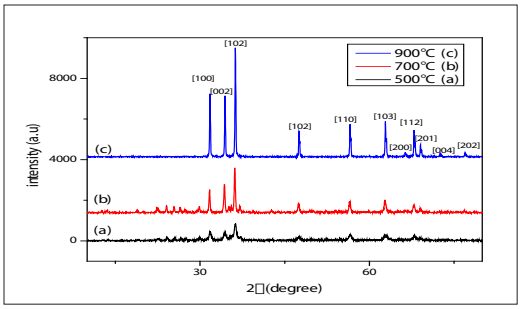

Figure 3: XRD diffractograms for 30% ALE concentration calcined at (a) 500 ˚C, (b) 700 ˚C and (c) 900 ˚C

The XRD pattern of 30% ZnO NPs calcined at 500, 700 and 900 ˚C are shown in Figure 3. XRD analysis was used to determine the crystalline phases of the ZnO NPs. Debye-Scherrer equation was used to determine crystallite size. Sample for 30% at 900 ˚C give distinctive Bragg reflection at 2θ value 31.78˚, 34.42˚, 36.25˚, 47.54˚, 56.58˚, 62.85 ˚, 66.33 ˚, 67.92 ˚, 69.06 ˚, 72.55˚ and 76.94˚ which are greatly showed the hexagonal wurtzite structure of ZnO NPs fully match with ZnO JCPDS 89-511. This shows sample 900 ˚C have high purity and crystalline nature of prepared due to hexagonal wurtzite structure. While for sample ZnO 30% annealing at temperature 700 ˚C and 500 ˚C show some minor impurities diffraction peaks observed in the XRD pattern indicated the present of Zinc Oxide sulfate ($Zn_3O(SO_4)_2$). Similar pattern was also obtained for concentration of ALE 40% and 50% where purity only obtained at 900 ˚C. This shows that concentration does not influence the purity of ZnO NPs. This supported by salahuddin et al., 2015 that give the same result.

Average crystalline size for temperature 500 ˚C is 24.19 nm while for ZnO NPS at 700 ˚C and 900 ˚C is 40.94 nm and 67.69 nm respectively. This results show that the higher the calcination temperature used, the larger the particle size produced. Moreover, increase the temperature apply to ZnO NPs would cause decrease value of FHWM as the diffraction peaks were also observed sharp due to the large particles sizes produce, the same result was reported by Salahuddin *et al.,* 2015. This further showed that calcination temperature played an importance role to determine the crystalinity and purity of ZnO NPs.

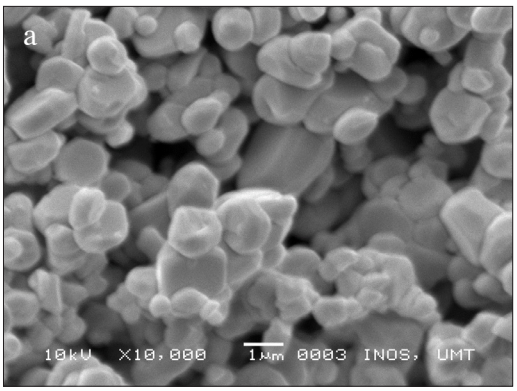

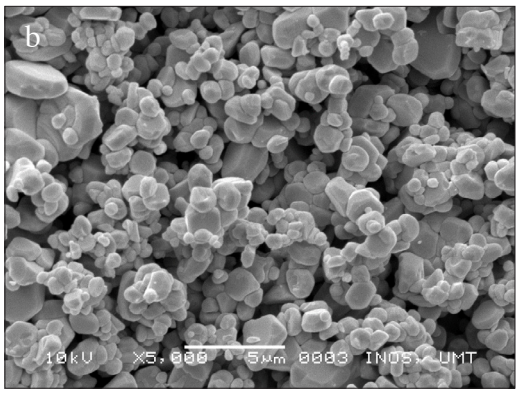

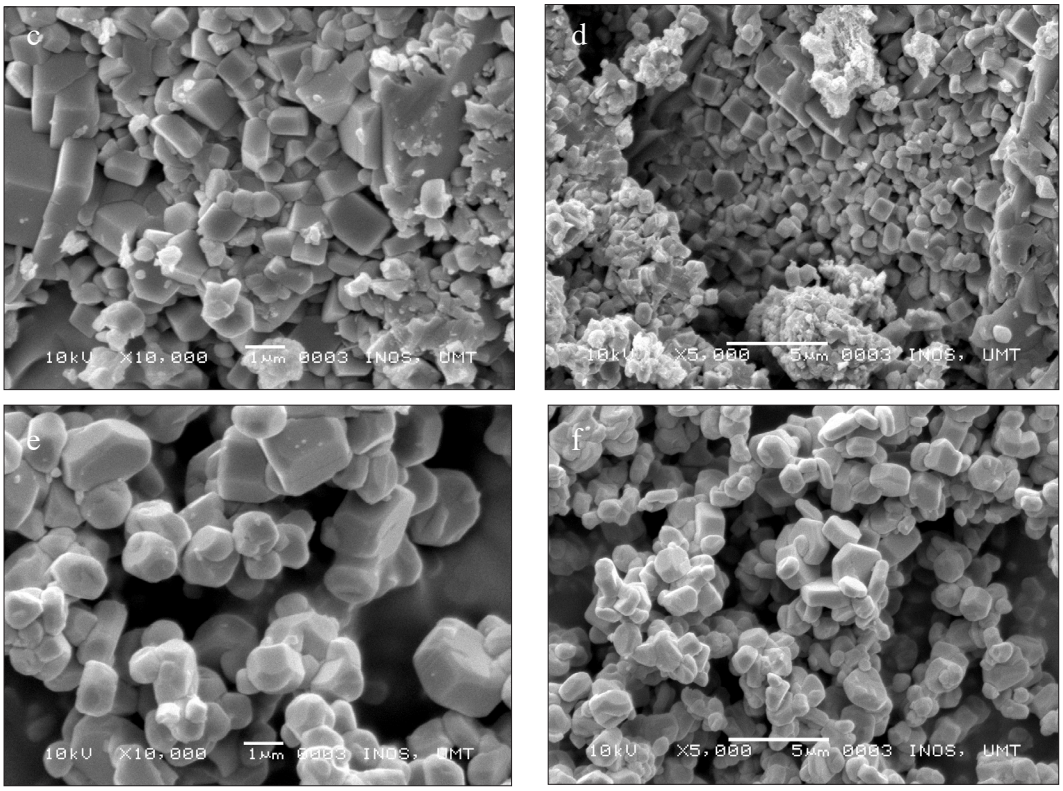

Figure 4: SEM images of ZnO NPs for ALE concentration of 30% at (a) 10000X and (b) 5000X, 40% (c) 10,000X and (d) 5000X, 50% (e) 10000X and (f) 5000X at 900 ˚C

Figure 4 show SEM image of ZnO Nps for concentration 30%, 40% and 50% at temperature 900 ˚C with magnification of 5000X and 10000X. Particle size for ZnO NPs with ALE 30% is from 100 nm to 400 nm while ZnO NPs with 40% ALE ranging from 140 nm to 900 nm and for ZnO NPs sample with 50% ALE is from 700 nm to 900 nm. This show that ZnO NPs with 50% ALE have higher particle size to be compared with 40% and 30% ALE and is in agreement with XRD results obtained. This result also showed that higher concentration of aloe vera extract used in the synthesis would also affect the particle size of ZnO NPs. According to Sanggetha *et al*., (2015) larger particle size would produce when using higher concentration of plant extract. For shape conformation, irregular shape was observed for sample 30% and 50% ZnO NPs, while for ZnO NPs 40% show slightly cube shape. Agglomeration was also observe due to high surface energy in ZnO NPs occur during synthesis in aqueous medium and presence of narrow spaces. between particles (Altaf et al., 2016).

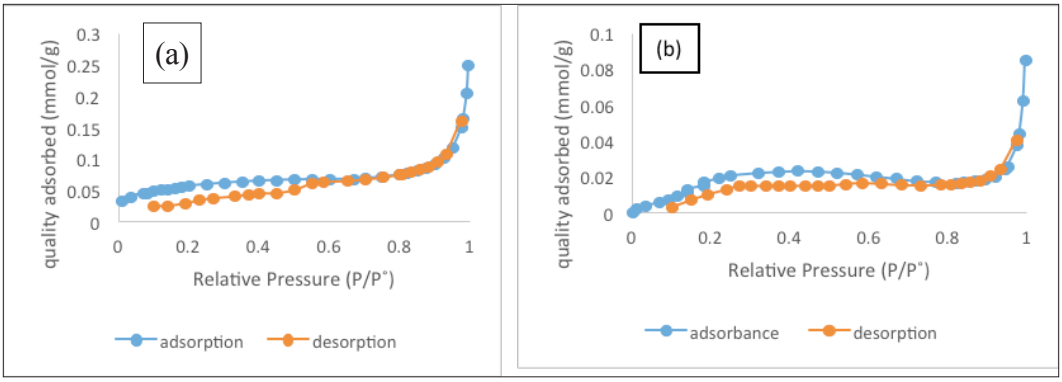

Figure 5: N_2 gas adsorption–desorption isotherms of ZnO NPs calcined at 900 ˚C using concentration of ALE at (a) 30% and (b) 40%

In this characterization, ALE concentration of 30% and 40% calcined at 900 ˚C was chosen due to the highest purity obtain in XRD analysis. Figure 5 shows graph of adsorption – desorption isotherms of ZnO NPs with ALE concentration of 30% and 40%. Both samples are type IV isotherm due to having hysteresis loop that work as connection with capillary condensation that indicated sample (a) and (b) are both mesopores. Reading from 0.6 P/P˚ to 0.2 P/P˚ for sample 30% while for sample 40% from 0.8 P/P˚ to 0.3 P/P˚ indicated that ZnO NPs are completely superposition during adsorption and desorption. At high pressure region (P/P˚ >0.7) for sample (a) and (P/P˚ >0.5) lag loop was observed due to the particles with internal voids of irregular shape and broad size distribution (Zhang *et al.,* 2012).

Even though, both sample show group IV pattern which indicate mesoporous structure (<50 nm), however both samples also have high relative pressure of P/P˚≈ 1, that indicated the presence of large pores which are more than (>50 nm) (Yu *et al.,* 2007). BET surface area for sample with 30% ZnO NPs 3.7038 m^2/g was recorded while sample 40% ZnO NPs is slightly lower with value of 2.0135 m^2/g. This shows that ZnO NPs 30% ALE have high surface area from ZnO NPs using 40% ALE. This finding is related with SEM images obtained that show ZnO NPs with 40% ALE have large particles size than ZnO NPs with 30% ALE.

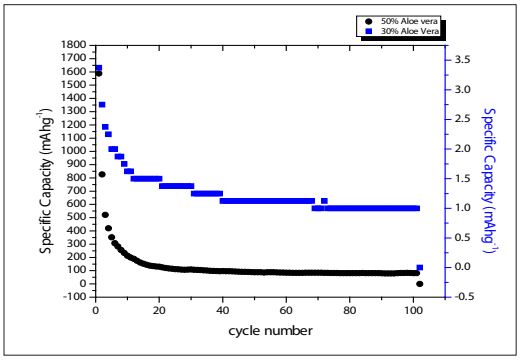

Figure 6: Cyclic performance for sample ZNO NPs using 30% and 50% ALE, calcined at 900˚C

The cyclic performances of ZnO NPs electrodes are shown in figure 6. The initial discharge capacity for ZnO NPs with 30% ALE is 1580 $mAhg^{-1}$ while for ZnO NPs with 50% ALE is 3.4 $mAhg^{-1}$ were recorded. For ZnO NPs exhibit the theoretical value of ZnO capacity is 978 $mAhg^{-1}$ and according to Zhang *et al.,* (2006) the excess capacity caused during discharge process, where the formation of solid electrolyte interphase (SEI) film on the particles occurs. SEI is important in lithium ion battery, this is because the function is to maintain cycling ability and prevent for further decomposition. Irreversible capacity occur due to the formation of Li_2O that show in equation (1).The initial irreversible capacity of ZnO NPs 30% and 50% ALE is 1.2 $mAhg^{-1}$ and 100 $mAhg^{-1}$ respectively.

$ZnO + 2Li \longrightarrow Zn + Li2O$ (1)

$Zn + Li \longleftrightarrow LiZn$ (2)

For stable reversible capacities 1 $mAhg^{-1}$ was recorded for ZnO Nps with 30% ALE while for sample of ZnO NPs with 50% ALE is at 80 $mAhg^{-1}$. Figure 6 show that sample ZnO NPs with 30% ALE have poorer capacity, this is due to the morphological of ZnO change during the formation LiZn that is shown in equation (2), resulting in the week performance of the electrode. Besides, weak performance of charge-transfer process between ZnO NPs and electrolyte might due to large band gap semiconductor that can contribute to poor capacity (Xiang *et al.,* 2006).

Conclusion

In this project, white powdered ZnO NPs has been successfully synthesized using different concentration of ALE (30%, 40% and 50%) and various temperatures (500 ˚C, 700 ˚C and 900 ˚C) calcined for 4 hours. The prepared ZnO NPs was successfully characterized by using Fourier – transform infrared spectroscopy (FTIR), Thermogravimetric Analysis (TGA), scanning electron microscopy (SEM), X-ray Diffraction (XRD) and Brunauer-Emmet and Teller (BET). Wavenumber from 400 cm^{-1} until 500 cm^{-1} was showed in FTIR spectra indicated the presence of Zn-O stretch. For TGA analysis only ZnO NPs 30% show a constant reading at 790 ˚C that indicated the loss of active components. The particle size of synthesis ZnO NPS for all concentration at 900 in the range between 100 nm until 900 nm. Irregular shape was observed in all three ALE concentration of ZnO NPs in SEM analysis. The shape was further proven by using XRD analysis that show hexagonal wutize structure was confirmed by matching and comparing JCPDS 89-511 and average particles size from 24.19 nm to 67.69 nm for all concentration and temperature by using Scherer's equation. ZnO NPs with 30% ALE showed large surface area and better volume (adsorption/desorption) in BET analysis. In cyclic performance study in lithium ion battery showed ZnO NPs 50% ALE have a good charge-transfer process to be compared with other samples.

Acknowledgements

Authors gratefully acknowledge Ministry of Higher Education, Malaysia, for their financial support through Fundamental research grant scheme (FRGS) (FRGS/1/2015/SG01/UMT/02/3).

References

Altaf, M., & Jaganyi, D. (2016). Characterization of Triangular Gold Nanoparticles UsingAloe arborescensLeaf Extract: A Green Synthesis Approach. Synthesis and Reactivity in Inorganic, Metal-Organic, and Nano-Metal Chemistry, 46(9), 1332-1335.

Ali, K., Dwivedi, S., Azam, A., Saquib, Q., Al-Said, M. S., Alkhedhairy, A. A., & Musarrat, J. (2016). Aloe vera extract functionalized zinc oxide nanoparticles as nanoantibiotics against multi-drug resistant clinical bacterial isolates. Journal of Colloid and Interface Science 472, 145-156

Bresser, D., Mueller, F. K., Fiedler, M., Krueger, S., Kloepsch, R., Baither, D., Winter, M., Paillard, E., Passerini, S. (2013). Transition-Metal-Doped Zinc Oxide Nanoparticles as a New Lithium-Ion Anode Material. Chemistry of Material, 25, 4977−4985

Espitia, P., Otoni, C., & Soares, N. (2016). Zinc Oxide Nanoparticles for Food Packaging Applications. Antimicrobial Food Packaging, 425-431

Hassan, H. S., Elkady, M. F., El-Sayed, E. M., Hamed, A. M., Hussein, A.M. (2018) Synthesis and characterization of Zinc Oxide Nanoparticles using green and chemical synthesis technique for phenol decontamination. Journal of Nanoelectronic and Material, 11, 179-194

Huang X. H, Xia. X. H, Yuan. Y. F, and Zhou. F. (2011) "Porous ZnO nanosheets grown on copper substrates as anodes for lithium ion batteries," Electrochimica Acta, vol. 56, no. 14, pp. 4960– 4965, 2011.

Iravani, S. (2011). Green synthesis of metal nanoparticles using plants. Green Chemistry, 13(10), 2638.

Jacobsson, T. J., Viarbitskaya, S., Mukhtar, E., & Edvinsson, T. (2014). A size dependent discontinuous decay rate for the exciton emission in ZnO quantum dots. Phys. Chem. Chem. Phys., 16(27), 13849-13857. doi:10.1039/c4cp00254g.

Liu, R., Duay, J., & Lee, S. B. (2011). Heterogeneous nanostructured electrode materials for electrochemical energy storage. Chem. Commun., 47(5), 1384-1404.

Salahuddin, N. A., El-Kemary, M., & Ibrahim, E. M. (2015). Synthesis and Characterization of ZnO Nanoparticles via Precipitation Method: Effect of Annealing Temperature on Particle Size

Sangeetha, G., Rajeshwari, S., & Venckatesh, R. (2011). Green synthesis of zinc oxide nanoparticles by aloe barbadensis miller leaf extract: Structure and optical properties. Materials Research Bulletin 46(12), 2560-2566.

Smijs, T., & Pavel. (2011). Titanium dioxide and zinc oxide nanoparticles in sunscreens: Focus on their safety and effectiveness. Nanotechnology, Science and Applications, 95.

Qi, W., Shapter, J. G., Wu, Q., Yin, T., Gao, G., & Cui, D. (2017). Nanostructured anode materials for lithium-ion batteries: Principle, recent progress and future perspectives. Journal of Materials Chemistry A, 5(37), 19521-19540.

Wan, H., Han, P., Ge, S., Li, F., Zhang, S., Li, H. (2018). Development Zinc Oxide–Cotton Fibers as Anode Materials for Lithium-Ion Batteries. International Journal of Electrochemical Science, 13, 4115 – 4122

Xiang, X., Zu, X. T., Zhu, S., Wei, Q. M., Zhang, C. F., Sun, K., & Wang, L. M. (2006). ZnO nanoparticles embedded in sapphire fabricated by ion implantation and annealing. Nanotechnology, 17(10), 2636-2640.

Xu, L., Bian, S., & Song, K. (2014). Graphene sheets decorated with ZnO nanoparticles as anode materials for lithium ion batteries. Journal of Materials Science, 49(18), 6217-6224.

Yang, C. C., Hung, Y. W., Lue, S. J. (2016). The carbon additive effect on electrochemical performance of LiFe0.5Mn0.5PO4/C composites by a simple solid-state method for lithium ion batteries. 2(18), 1-1.

Yu, J., Zhang, L., Cheng, B., & Su, Y. (2007). Hydrothermal Preparation and Photocatalytic Activity of Hierarchically Sponge-like Macro-/Mesoporous Titania. The Journal of Physical Chemistry C,111(28), 10582-10589.

Zhang, L., Jiang, Y., Ding, Y., Povey, M., & York, D. (2006). Investigation into the antibacterial behaviour of suspensions of ZnO nanoparticles (ZnO nanofluids). Journal of Nanoparticle Research, 9(3), 479-489.

Zhang, Y., Li, Q., Jia, J., & Meng, A. (2012). Thermodynamic analysis on heavy metals partitioning impacted by moisture during the MSW incineration. Waste Management, 32(12), 2278-2286.

Universiti Malaysia Terengganu Journal of Undergraduate Research *eISSN: 2637-1138*
Volume 2 Number 2, April 2020: 9-14

SYNTHESIS AND CHARACTERIZATION OF TiO_2/ZnO-EPOXY BEADS AND THEIR PERFORMANCE FOR THE DEGRADATION OF DYE

MOHAMAD HANIF AKMAL HUSSIN, WAN RAFIZAH WAN ABDULLAH, MOHAMAD AWANG[1] AND WAN SALIDA WAN MANSOR*

Faculty of Ocean Engineering Technology and Informatics, Universiti Malaysia Terengganu, Terengganu, Malaysia

**Corresponding author: wansalida@umt.edu.my*

Abstract: Semiconductor oxides such as titanium dioxide (TiO_2) and zinc oxide (ZnO) are used as the photocatalyst for removing contaminants. In addition, TiO_2 and ZnO nanoparticles in the suspension form makes it difficult to be recovered and recycled. This study was conducted to investigate the efficiency of immobilizing TiO_2 and ZnO nanoparticles in epoxy beads. The immobilization process using different ratios of photocatalysts TiO_2/ZnO (1:0, 3:1, 1:1, 1:3 and 0:1) fixed on epoxy material. These epoxy beads were used for dye removal in photocatalysis using methylene blue (MB) solution at a concentration of 10mg/L. Besides, epoxy beads also characterized using scanning electron microscope (SEM), attenuated total reflection Fourier-transform infrared (ATR-FTIR) spectroscopy and thermogravimetric analysis (TGA). The results showed that the highly recommended epoxy bead is 3:1 ratio of TiO_2/ZnO because it has good performance in dye degradation that proved from reducing concentration of MB to 2.4mg/L (76%). However, TiO_2/ZnO characterization of 3:1 by SEM show on the surface the particle are found to be spherical in shape which is relatively high efficiency for the degradation, ATR-FTIR pattern in broad band 4000 cm^{-1} - 400cm^{-1} which correspond to hydroxyl stretching to be adsorbed at peak (474.49 cm^{-1} - 3722.61cm^{-1}) respectively to the optimum for the degradation and TGA rate of change are 5mg to 2.5mg that residue (49.78%) due to decomposition or oxidation from mass loss. These findings are very effective and economical technique to be cost saving and highly efficient photocatalyst.

Keywords: Photocatalysis, titanium dioxide, zinc oxide, immobilization, Epoxy beads

Introduction

Photocatalyst is a process where light and catalyst were concurrently used to support and speed up a chemical reaction. So, photocatalyst was defined as the acceleration of photoreaction by the present of catalyst. Photocatalyst was divided into two categories which are a homogeneous and heterogeneous photocatalytic process (Rehman *et al.,* 2009). Homogeneous photocatalytic process mostly used with metal complete as the catalyst like iron, chromium and copper. In this process under the photon and thermal condition, the higher oxidation stated of metal ion complexes generated hydroxyl radicals. These hydroxyl radicals reacted with organic matter which leads destruction of toxic matters. While the heterogeneous photocatalytic process is a technically gifted method that used for degradation of various organic pollutants in wastewater (Rajeshwar *et al.,* 2008). This process has a few advantages over competing processes which are complete mineralization, no waste disposal problem, low cost and necessity of mild temperature and pressure condition only.

Heterogeneous photocatalysis employing semiconductor catalysts has demonstrated its efficiency in degrading a wide range of organics into readily biodegradable compounds. The ideal photocatalyst should possess the following properties such as nontoxic, costless, photoactive, sustainable towards visible or near UV light and biologically and chemically inert (Khan *et al.,* 2015).